Global Change Biology (2005) **11,** 2041–2056, doi: 10.1111/j.1365-2486.2005.01028.x

TECHNICAL ADVANCE

Theory and performance of an infrared heater for ecosystem warming

B. A. KIMBALL

U.S. Water Conservation Laboratory, USDA, Agricultural Research Service, 4331 East Broadway Road, Phoenix, AZ 85040, USA

Abstract

In order to study the likely effects of global warming on future ecosystems, a method for applying a heating treatment to open-field plant canopies (i.e. a temperature free-air controlled enhancement (T-FACE) system) is needed which will warm vegetation as expected by the future climate. One method which shows promise is infrared heating, but a theory of operation is needed for predicting the performance of infrared heaters. Therefore, a theoretical equation was derived to predict the thermal radiation power required to warm a plant canopy per degree rise in temperature per unit of heated land area. Another equation was derived to predict the thermal radiation efficiency of an incoloy rod infrared heater as a function of wind speed. An actual infrared heater system was also assembled which utilized two infrared thermometers to measure the temperature of a heated plot and that of an adjacent reference plot and which used proportional–integrative–derivative control of the heater to maintain a constant temperature difference between the two plots. Provided that it was not operated too high above the canopy, the heater system was able to maintain a constant set-point difference very well. Furthermore, there was good agreement between the measured and theoretical unit thermal radiation power requirements when tested on a Sudan grass (*Sorghum vulgare*) canopy. One problem that has been identified for infrared heating of experimental plots is that the vapor pressure gradients (VPGs) from inside the leaves to the air outside would not be the same as would be expected if the warming were performed by heating the air everywhere (i.e. by global warming). Therefore, a theoretical equation was derived to compute how much water an infrared-warmed plant would lose in normal air compared with what it would have lost in air which had been warmed at constant relative humidity, as is predicted with global warming. On an hourly or daily basis, it proposed that this amount of water could be added back to plants using a drip irrigation system as a first-order correction to this VPG problem.

Key words: canopy temperature, ecosystems, energy balance, evapotranspiration, global change, global warming, infrared heater, microclimate, thermal radiation, wind speed

Received 27 January 2005; revised version received and accepted 4 May 2005

Introduction

The concentrations of carbon dioxide (CO_2) and several other radiatively active gases are increasing in the atmosphere, and atmosphere-ocean general circulation models have predicted a consequent global warming (IPCC, 2001). Both the higher levels of CO_2 directly and any warming will likely affect the growth of plants. Therefore, a high priority in global change research is to develop a predictive knowledge of what the probable consequences will be for both managed and natural ecosystems. In addition, because plant growth removes CO_2 from the air with the potential to sequester some of it in their own tissues and in soil organic matter, another high priority is to establish the amount of sequestration possible under various environmental conditions and management practices, and thereby mitigate the rise of atmospheric CO_2.

The effects of elevated CO_2 and increased temperature on plants have been studied for centuries in various types of chambers and greenhouses (e.g. Drake *et al.*,

Correspondence: Dr Bruce A. Kimball, tel. + 602 437 1702x248, fax + 602 437 5291, e-mail: bkimball@uswcl.ars.ag.gov

1985). Such research has produced considerable knowledge about the effects of both CO_2 and temperature on plant growth. However, the chambers themselves affect the growth of the plants because of drastically changed air flow and shading compared with outside (e.g. Kimball *et al*., 1997). Moreover, the scale of chambers is generally not large enough to reproduce the interactive effects among plants and produce a realistic plant canopy with ecosystem processes (e.g. McLeod & Long, 1999). Therefore, in order to increase our confidence about the effects of elevated CO_2 and temperature on plant growth, there is a need to conduct manipulative experiments under free-air open-field natural conditions.

Technology for exposure of plants to elevated levels of CO_2 and other trace gases under field conditions has been developed (e.g. Hendrey, 1993), and many subsequent experiments have been conducted or are underway (e.g. Kimball *et al*., 2002; http://cdiac.esd.ornl.gov/programs/FACE/face.html). In contrast to elevating gas concentrations under free-air conditions, elevation of air temperature at the ecosystem scale is more problematic. An ideal experimental system for global change ecosystem research would create environmental conditions like those predicted by the climate models to occur at some time in the future. The IPCC (2001) estimates that radiative forcing will increase by 4–9 $W m^{-2}$ by the end of this century depending on radiative gas emissions scenario. In turn, they project that this small increase in forcing (small compared with the 100–400 $W m^{-2}$ of thermal radiation coming down from the sky and the 1000 $W m^{-2}$ of solar radiation at noon on a clear day) will cause an increase in global mean air temperatures ranging from about 1.5 to 6.0 °C depending on scenario and climate model used. From a plot-scale experimental point of view, therefore, ideally the air upwind from our plots should be warmed and humidified by an amount representative of the future global warming while the sky thermal radiation is increased 4–9 $W m^{-2}$.

Global warming is also expected to cause overall increases in evaporation from the oceans with consequent greater precipitation on average world wide but with uncertain changes in patterns of distribution of the precipitation (IPCC, 2001). Another aspect however, is that *absolute* humidity of the air is expected to increase, although *relative* humidity is expected to remain more or less constant. Therefore, the ideal experimental system should both heat the air and humidify it so as to maintain constant relative humidity. If the experimental apparatus only heats the air, then the vapor pressure gradients (VPGs) from inside the leaves to the air will not be representative of those predicted in the future, and consequently, neither will the rates of transpiration and soil water depletion. On the other hand, if a means could be found to heat the vegetation by the amounts expected in the future while compensating for the changes in water vapor pressure from inside the plant to the outside air, this alternative system would be attractive if it were economical.

Several attempts have been made to heat ecosystem vegetation and/or soil without heating the air (e.g. Shaver *et al*., 2000; Shen & Harte, 2000). Soil warming cables or tubes have been used (e.g. Hillier *et al*., 1994; Ineson *et al*., 1998), which offer opportunities for studying the effects of temperature on soil processes, but plant canopy temperatures are largely uncoupled from soil temperatures except for very short vegetation. An inadvertent canopy temperature treatment was reported by Pinter *et al*. (2000), who detected that the blowers used in their free-air CO_2 enrichment experiments increased canopy temperatures compared with blower-less control plots at night because of mixing of cooler canopy air with warmer air aloft. A similar but deliberate canopy temperature treatment is being achieved by researchers on the VULCAN Project (http://www.vulcanproject.com/), who are deploying covers over their plots at night to reduce infrared radiant loses. However, both of the latter treatments are strictly night-time only with little control over the treatment conditions achieved.

One approach which has appeal is warming the vegetation with infrared heaters deployed above the canopy. It is appealing because the warming should be similar to normal solar heating of the leaves, and it should be energetically efficient because one would heat the leaves directly without having to overcome a boundary layer resistance if the air were heated first. Harte & Shaw (1995) and Harte *et al*. (1995) apparently were the first to utilize infrared heaters (Table 1). Starting in 1991 on montane vegetation, their experiment is continuing as of the date of this writing. They use the heaters in a constant power mode (+ 22 $W m^{-2}$ above ambient), which they justified in part because global warming likely is being driven by an increase in downward thermal radiation. However, 22 $W m^{-2}$ is much more than the 4–9 $W m^{-2}$ projected for the future climate forcing (IPCC, 2001), and yet as shown by several prior researchers (Table 1) and as will be shown in this paper, for much of the time and especially under normal daytime unstable atmospheric conditions, far more thermal energy than 22 $W m^{-2}$ is required to produce the projected amounts of future warming of ecosystem vegetation.

An improvement in infrared heater control was made by Nijs *et al*. (1996), who varied the heat output in order to maintain a constant 2.5 °C difference in canopy temperature for a 3-week trial between a treated and a control plot of ryegrass (*Lolium perenne*). More recent

Table 1 Heater capacity, thermal radiation fluxes, thermal radiant efficiency, and ecosystem responses reported for several infrared-heating experiments

Investigators	Ecosytem	Infrared heater electrical power rating (W)	Heater height above soil surface (m)	Heated plot area (m^2)	Thermal radiation flux ($W\,m^{-2}$)	Thermal radiant efficiency (%)	Microclimatic effect
Harte *et al*. (1995)	Montane	1500	2.5	10	22	15	Up to 3 °C increase in soil temperature
Nijs *et al*. (1996)	Ryegrass	3000	~ 1.0	0.2	–	–	2.5 °C increase in leaf temperatures at 0.5 canopy height
Bridgham *et al*. (1999) and Noormets *et al*. (2004)	Bog and fen	1500	1.3	2.1	76–104	11–15	1.6–4.1 °C increase in soil temperature at 15 cm depth
Wan *et al*. (2002)	Tall grass prairie	1500	1.5	4.0	100	27	2.0–2.6 °C increase in soil temperature. Daily maximum air temperatures in canopy increased 0.1 °C and minimums increased 2.3 °C at night
Shaw *et al*. (2002)	Grassland	–	–	3.1	80	–	0.8–1.0 °C increases in soil and plant canopy temperatures

Thermal radiant efficiency was calculated as the percentage of electrical power input that resulted in useful thermal radiation impinging on the vegetation.

reports of infrared heaters for ecosystem warming include Bridgham *et al*. (1999), Luo *et al*. (2001), Shaw *et al*. (2002), Wan *et al*. (2002), and Noormets *et al*. (2004). However, none of the above researchers have addressed the VPG problem.

Several reports, but especially Wan *et al*. (2002), present data characterizing the canopy microclimate under infrared heating. It is the purpose of this report to provide theory and additional data about the performance of infrared heating, which could be used to aid in the design of future temperature free-air controlled enhancement (T-FACE) heating systems. I will also propose a method to compensate for the altered plant-air water VPG.

Infrared heater and control system description

An infrared heater was purchased similar to the ones used by Harte *et al*. (1995), Bridgham *et al*. (1999), and Wan *et al*. (2002) (Table 1). The heater is a 2000 W, 240 V Model HS-2420 from Kalglo (Trade names and company names are included for the benefit of the reader and do not imply any endorsement or preferential treatment of the product listed by the authors or the U. S. Department of Agriculture.) Electronics Co. Inc. (Bethlehem, PA, USA) (Figs 1d and e), which is physically the same size as those of the other authors but has a higher capacity than their 1500 W model. The housing of the unit is 165 cm long and has an equilateral triangle cross-section (14 cm on a side), except the lower side is a concave polished reflector. A rod-shaped heating element (8 mm diameter × 151 cm long) is mounted at the focal point of the polished aluminum reflector. The outer emitting surface of the heating element is a sheath made of an iron-nickel alloy (incoloy 800), which has been annealed and is somewhat oxidized, which likely affected its emissivity for thermal radiation (B. MacDoughall, Kalglo Electronics, personal communication, 17 November 2004).

Similar to Nijs *et al*. (1996), a proportional–integrative–derivative (PID) control system was assembled to enable maintenance of a controlled temperature rise of a heated plot over that of a similar control plot (Fig. 1e). The temperature under the heater and that of the control plot were sensed using infrared thermometers (IRTs, Model IRTS-P5, Apogee Instruments Inc., Logan, UT, USA). The IRTs had previously been carefully calibrated over a wide range of target (−5 to +70 °C) and ambient (i.e. instrument body, 3–45 °C) temperatures using an extended area calibration source (Model 100-06/CF, Electro Optical Industries, Santa Barbara, CA, USA) in a controlled-temperature room. According to the manufacture, the IRTs are sensitive to radiation within 6.5 to 14μm, a waveband over which both the

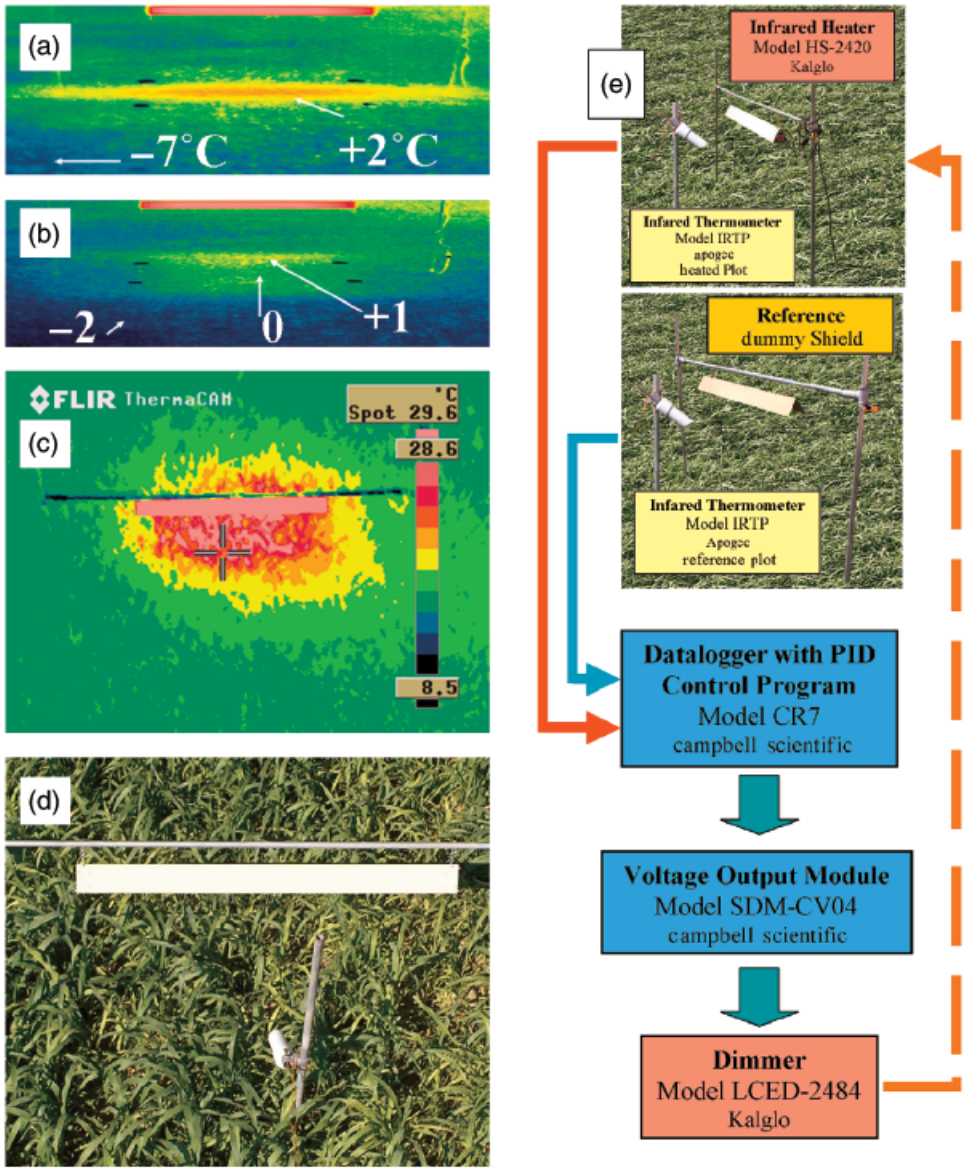

Fig. 1 (a) Thermal image of heating pattern produced by infrared heater on mown lawn before dawn on 6 February 2003. The pink rectangle at the top of the image is the heater itself. The black spots are aluminum blocks (which have low emissivity and therefore appear cold) spaced 1 m apart on either side of the heater and even with the ends of the heater. (b) Thermal image produced on same lawn before dawn on 7 February 2003 after modification of the heater's reflector per Harte *et al*. (1995). (c) Thermal image of heating pattern in 114 cm tall Sudan grass (*Sorghum vulgare*) obtained before dawn on 15 August 2004. (d) Normal visible light image of heater and an infrared thermometer deployed over 55 cm tall Sudan grass near noon on 27 September 2004. (e) Schematic diagram of infrared heating system with infrared heater, infrared thermometers over the heated and reference plots, datalogger, voltage output module, and dimmer, which regulates the heater.

sky and the infrared heater emit radiation that can be reflected from the plant canopy to the IRTs. Therefore, for the retrospective analyses used to produce the measured heater system performance data presented in this paper, the temperatures sensed by both IRTs were corrected for sky radiation, and the one over the heated plot for reflected heater radiation assuming a canopy reflectance of 2%.

The IRT signals were measured using a datalogger (Model CR7, Campbell Scientific, Logan, UT, USA), which also served as the PID controller. Connected to the datalogger (The CR7 datalogger required an SDM upgrade to be compatible with the SDM-CVO4, whereas newer Campbell loggers are already compatible.) was a Model SDM-CVO4 Current/Voltage Output Module (Campbell Scientific), which produced a

0–10 V signal with which to control the heater. This signal was fed to a Model LCED-2484 Dimmer (Kalglo Electronics Co. Inc.), which in turn regulated the output of the heater by modulating a portion of a 1/60th second duty cycle.

Starting with an initial draft of a PID controller program obtained from Campbell Scientific, it was modified to suit our heater system with two IRT input signals. Then following Williams (2003), the system was tuned, settling on 50, 0.005, and 20 for the proportional, integrative, and derivative coefficients, respectively. Thus, the CR7 datalogger was able to produce a PID signal to control the heater to maintain a set temperature difference between the heated and control plots.

Several tests were conduced of the heater and PID control system, including 21–22 September 2004, when the heater was operated under PID control over 1 m tall Sudan grass. Another test of the heater over second crop 0.6 m tall Sudan grass was conducted on 30 September 2004, when the heater was operated at constant full power (i.e. no PID control). Ancillary weather data consisting of solar radiation (pyranometer, Model 8-48 Eppley Laboratory, Newport, RI, USA) wet and dry bulb temperatures at 2 m (psychrometer, Peresta *et al*., 1991), and wind speed at 2 m above the soil (generator-type cup anemometer, Model 12102, R.M. Young Co., Traverse City, MI, USA) were measured in the field a few meters away from the heater.

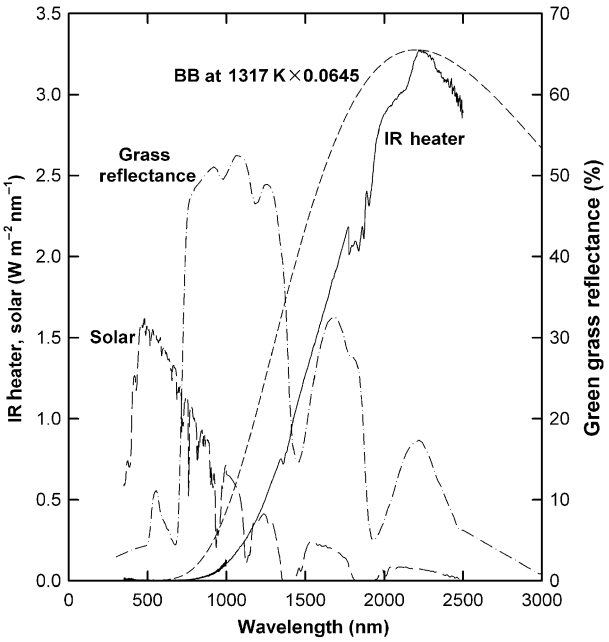

Fig. 2 Irradiance spectrum for Model HS-2420 Kalglo Electronics infrared heater operated at 2000 W adjusted to the position of the heater element surface. Also shown is the irradiance spectrum for a black body at 1317 K computed from Planck's Law (e.g. Campbell, 1977), which peaks at the same wavelength as the heater, times 0.0645 to make the peaks the same height. Solar radiance outside the building taken with the same instrument near noon on the same July day is presented for comparison purposes. Also plotted is the reflectance spectrum for a green grass surface (from Jet Propulsion Laboratory Spectrum Library, http://speclib.jpl.nasa.gov/scripts/lib/asp/buildhtm.asp?DB=vegetation&ID=4).

Theory and performance

Heating pattern

The heating pattern produced by the heater was determined using a thermal imager (Model SC2000 ThermaCAM, Flir Systems, Danderyd, Sweden). The pattern over a short grass lawn by the heater as delivered from the factory was a rather narrow strip (Fig. 1a). Therefore, the reflector was modified to make it less concave following Harte & Shaw (1995), which consisted of removing the reflector, cutting off a strip 21.5 mm wide, and replacing it. The modified heater produced a much more uniform heating pattern (Figs 1b and c), and all subsequent testing was performed using the modified heater. At a height of 1.5 m over the lawn (Fig. 1b) the heated area was about 2 m transverse to the heater and 1.5 m longitudinally. When 60 cm above a Sudan grass (*Sorghum vulgare*) canopy, the heated area was about 1 m wide and 1.5 m long (Figs 1c and d). Thus, with the modified reflector, the angle over which the radiation was dispersed downward was about 67°.

The amount and pattern of shading of solar radiation by the heater's housing varied with sun angle, of course, but if the sun were at zenith, the proportion of shading of the heated area would amount to 8% or 15% at heights above the vegetation of 1.5 or 0.6 m, respectively. For the heater control system to work properly (Fig. 1e), it was essential to have the shading from the heater and that from the dummy shield be as identical as possible, and similarly, to have the target areas of the infrared thermometers be the same to be sure they viewed the same amounts of shading.

Spectral irradiance

In order to be useable for this ecosystem global warming application, an infrared heater should emit radiation only in the thermal part of the spectrum and none at wavelengths less than about 850 nm, which may be photochromatically active (e.g. Salisbury & Ross, 1992, Chapter 20). Harte *et al*. (1995) reported that their 1500 W heater emitted no visible radiation. However, our 2000 W model glowed slightly red to our eyes when fully on, but not at half power. To

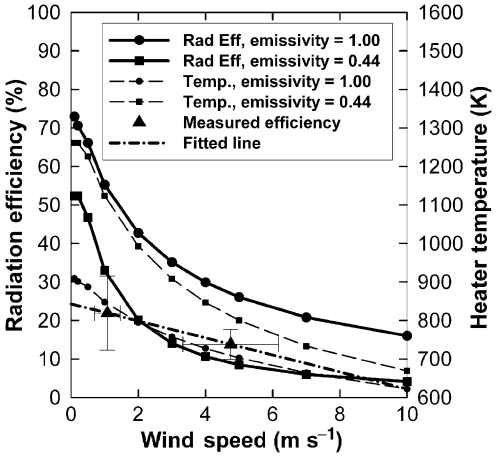

Fig. 3 Theoretical radiation efficiencies of the heating element (8 mm diameter, 1.5 m long) of an infrared heater (2000 W), vs. wind speed for emissivities of the element of 1.00 (black body) and 0.44. Radiation efficiency is defined as the percentage of the input electrical energy moving away from the heating element in the form of thermal radiation. Also shown are the corresponding heating element temperatures. The measured points were obtained using the up-looking long-wave sensor on a Kipp & Zonen CNR1 net radiometer on a breezy (wind measured at 2 m height) afternoon (29 September 2004) and at dawn on a clear calm morning (1 October 2004). The fitted line is Eq.7.

measure the actual spectral reflectance of the heater at full power, it was deployed at a height of 1.5 m above the concrete floor of a machine shop whose windows were covered. A white spectralon reflectance plate (reflectance = 99%) was placed on the floor under the center of the heater. Then, with the sensor head about 64 cm above the plate, a recently calibrated spectral radiometer (Model ASD-FR (full range) Analytical Spectral Devices, Boulder, CO, USA) was used to determine the spectral irradiance of the heater from 350 to 2500 nm. For comparison purposes, the spectral radiance of the sun outside the building near noon on that day (8 July 2004) was also obtained.

To also determine the time constant of the heater, the spectral measurements were taken at 0, 2, 4, 7, 15, and 21 min after turning on the heater. These data showed the time constant of the heater was 2.5 min (i.e. after 2.5 min, $1-\exp(-1) = 0.632$ of the total temperature rise of the heater had occurred).

The irradiance spectrum of the heater shows very little energy being emitted below 850 nm (Fig. 2), which implies that it ought not be photochromatically active (e.g. Salisbury & Ross, 1992, Chapter 20). Therefore, plants ought not 'see' it but only be warmed by it, so it should be suitable for the ecosystem warming application. However, the incoloy-heating element is neither black nor grey, as indicated by the large departure of the spectrum from that of a black body.

Total long-wave down-coming radiation and efficiency

The heater was deployed in the field at 60 cm above a Sudan grass canopy (Figs 1d and e). A net radiometer (Model CNR1, Kipp & Zonen, Delft, the Netherlands) was mounted on an arm that could be rotated so as to move the sensor head in a horizontal plane at 30 cm below the heating element and varying distances horizontally away. The Model CNR1 actually has 4 separate sensors for up- and down-going short- and long-wave radiation. For this test, only the up-looking long-wave sensor (equivalent to a Kipp & Zonen Model CG3 pyrgeometer) was utilized. According to the manufacturer, this sensor has a 4.5 to 42 μm sensitivity band, which corresponds well with typical Earth surface temperatures. However, the heating element of the infrared heater operates at a temperature of about 550°C (see next section), and at this hotter temperature only 0.574 of the radiation that would be emitted by a black body is within 4.5 to 42 μm waveband. Therefore, the values from the CNR1 sensor were adjusted by dividing by 0.574. On a breezy afternoon (29 September 2004) and again before dawn on a clear calm CRN1 morning (1 October 2004), the radiometer was moved in 5 cm increments from beneath the heater to long distances away on both sides and back again.

On the calm morning (wind speed at 2 m height averaged 1.08 m s^{-1} over the 2.5 h measurement period (SD = 0.38 m s^{-1} based on 15 min averages), the measurements averaged 577 W m^{-2} over about 0.76 m^2 of area in the horizontal plane of the sensor, which amounted to 438 W of useful thermal radiation emitted by the heater. For an electrical power input of 2000 W, therefore, the thermal radiant efficiency was only about 22% under these fairly calm conditions (Fig. 3). On the breezy afternoon (average wind speed = 4.75 m s^{-1} (SD = 1.42)), the useful output was even lower (275 W), and the efficiency was only 14%.

Heater element temperature and thermal emissivity

A type-K thermocouple connected to a hand-held electronic thermometer (Model 54II, Fluke Corp., Everett, WA, USA) was used to measure the temperature of the heater element on a relatively calm, partly cloudy day in the field. Wearing gloves, the thermocouple was pressed against the heater element as tightly as its lead wire would allow without bending when the heater was full-on (2000 W). The lower portion of the element was about 500 °C, whereas the upper portion, which was within view of the reflector and more sheltered from the wind was hotter, about 600 °C.

For a black body at 550 °C, the thermal radiation emitted would be 26 000 W m^{-2} (Stephan's Law, e.g.

Kimball, 1981). Taking the 438 W of thermal radiation for relatively calm conditions from the previous section, and distributing it over the surface area of the heating element ($\pi \times 0.008$ m diameter $\times$ 1.52 m long = 0.0382 m^2), the radiant emitted flux was 11,500 W m^{-2}. Therefore, the overall effective emissivity of the heater element plus reflector systems was about 0.44.

Theoretical heater efficiency in nonstill air

Sales literature from the manufacturer targets warming of farrowing pens and other in-door heating applications. However, use of infrared heaters in free-air open-field conditions implies exposure of the heater to wind and concomitant forced convection. Therefore, a simple model was developed to illustrate the effects of wind on the thermal infrared efficiency of the heater used in this study (which would not apply to other designs with different geometries or with covers or shields over the emitting surface). Although the housing would restrict airflow over the top, the heating element is basically an 8 mm diameter $\times$ 1.5 m rod suspended in air.

At the surface of the rod, the electrical power in ($\mathbf{P}_h$, W) equals the power radiated ($\mathbf{R}_h$, W m^{-2}) and convected ($\mathbf{H}_h$, W m^{-2}) away per unit surface area (A, m^2).

$$\mathbf{P}_h/A = \mathbf{R}_h + \mathbf{H}_h. \quad (1)$$

From Stephan's Law,

$$\mathbf{R}_h = \varepsilon_h \sigma (T_h + 273.15)^4, \quad (2)$$

where ε_h is effective emissivity of heater element surface; σ is the Stephan–Boltzmann constant (5.6697×10^{-8} W m^{-2} K^{-4}); T_h is the temperature of heater surface (°C).

$$\mathbf{H}_h = \rho c_p (T_h - T_a)/r_a, \quad (3)$$

where ρ is the air density (kg m^{-3}); c_p is the air heat capacity at constant pressure (J kg^{-1} C^{-1}); T_a is the air temperature (°C); r_a is the aerodynamic resistance (s m^{-1}), which can be calculated for forced convection from $r_a = 307(d/u)^{0.5}$ (Campbell, 1977, Eqn (6.15)) and for natural convection at low wind speeds from $r_a = 840[d/(T_h - T_a)]$ (Campbell, 1977, Eqn (6.25)), where u is windspeed (m s^{-1}) and d is the heating element rod diameter.

Linearizing following Kimball (1981),

$$\mathbf{R}_h \approx \mathbf{R}_h^o + \delta_h (T_h - T_h^o), \quad (4)$$

where δ_h is $4\varepsilon_h \sigma (T_h^o + 273.15)^3$ and $\mathbf{R}_h^o$ is the thermal radiation calculated using an initial guess T_h^o for T_h in Eqn (2). Rearranging and solving for T_h

$$T_h = \frac{[(\mathbf{P}_h/A) - \mathbf{R}_h^o + \delta_h T_h^o + (\rho c_p/r_a)T_a]}{[\delta_h + (\rho c_p/r_a)]}. \quad (5)$$

Starting with an initial guess for T_h^o, computing an estimate for T_h, and then successively using T_h estimates for T_h^o in an iterative fashion, Eqn (5) quickly converges to a value for T_h that satisfies Eqn (1), and then $\mathbf{R}_h$ and $\mathbf{H}_h$ can be calculated from Eqns (2) and (3).

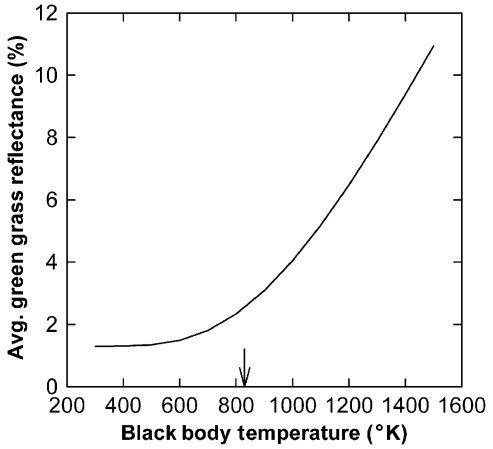

Fig. 4 Average reflectance of green grass to radiation emitted from a black body as a function of temperature of the black body. The arrow indicates the average measured temperature (550 °C) of the heating element of our infrared heater.

Defining the radiation efficiency of the infrared heater as the percentage of the energy emitted as thermal radiation, the efficiency (η_h, %) is:

$$\eta_h = 100[\mathbf{R}_h/(\mathbf{P}_h/A)]. \quad (6)$$

If the heating element were a black body, it would have an upper radiation efficiency of about 72% in still air (Fig. 3). However, as wind speed increases, efficiency drops rapidly with increasing wind speed to be only about 16% at 10 m s^{-1}. Corresponding temperatures of the heating element are about 900 and 600 K (Fig. 3). For the case of our heater, for which the overall emissivity was determined to be about 0.44, the maximum theoretical still-air efficiency would be about 52%, decreasing to only about 4.1% at a wind speed of 10 m s^{-1}. Correspondingly, heating element temperatures for an emissivity of 0.44 are much hotter compared with those for a black body, decreasing from about 1300 to 700 K as wind increases from 0 to 10 m s^{-1}.

The efficiency curve for 0.44 emissivity passes between the two measured points (Fig. 3). However, the correct wind speed for the theoretical curves likely was not the 2 m measured wind speed as used for the measured points because of the differences in elevation above the ground surface between the anemometer and the heater and also especially because the housing changes the wind flow over the heating element. Although it would be desirable to have a theoretical equation that perfectly describes the efficiency of an infrared heater, nevertheless, it is encouraging that the

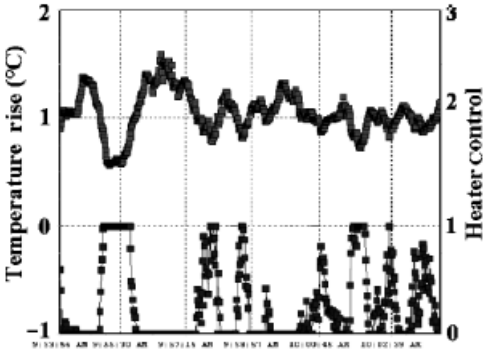

Fig. 5 Snapshot of computer screen showing the second to second temperature rise of plot of 95 cm-tall Sudan grass heated by an infrared heater above that of an unheated reference plot. The full width of the time axis is 10 min. Also shown is the corresponding heater control signal (scaled from 10 to 1), where 0 indicates the heater was off and 1 indicates it was fully on. The 2000 W heater was 60 cm above the top of the canopy.

curve for 0.44 emissivity is as close as it is, almost passing through the standard deviation range of the two points. The 'fitted line' was obtained by fitting a line to the measured points, although a constant value of 18% would fall within the scatter of the data

$$\eta_h(\%) = 24.8 - 2.21u. \quad (7)$$

Average reflectance of vegetation to black body radiation

While the infrared heater did not emit any significant radiant energy at wavelengths shorter than about 800 nm, it did emit in the near-infrared portion of the spectrum (Fig. 2). Because vegetation is up to about 50% reflective in the near infrared (Fig. 2, right scale for green grass reflectivity, from Jet Propulsion Laboratory (JPL) Spectrum Library, http://speclib.jpl.nasa.gov/scripts/lib/asp/buildhtm.asp?DB=vegetation&ID=4), the possibility existed that the high reflectivity in this portion of the spectrum would reduce the effectiveness of infrared heaters for warming vegetation. Using Planck's Law (e.g. Campbell, 1977, p. 50), the thermal radiant emission of a black body at small wave length intervals over a range of operating temperatures was calculated, which then was multiplied by the corresponding green grass reflectance (Fig. 2). The published reflectance spectrum from JPL extends to 14 000 nm, and for longer wave lengths than this, a constant, near-black-body reflectance of 1.5% was assumed.

The resultant calculated effect of the high near-infrared reflectance for vegetation (Fig. 2) on the overall average reflectance was minor (Fig. 4). At very cool temperatures, it was 1.5%, rising to just over 2% for the 550 °C (= 823 K in Fig. 4) temperature of the heating element of the infrared heater. For a relatively hot body

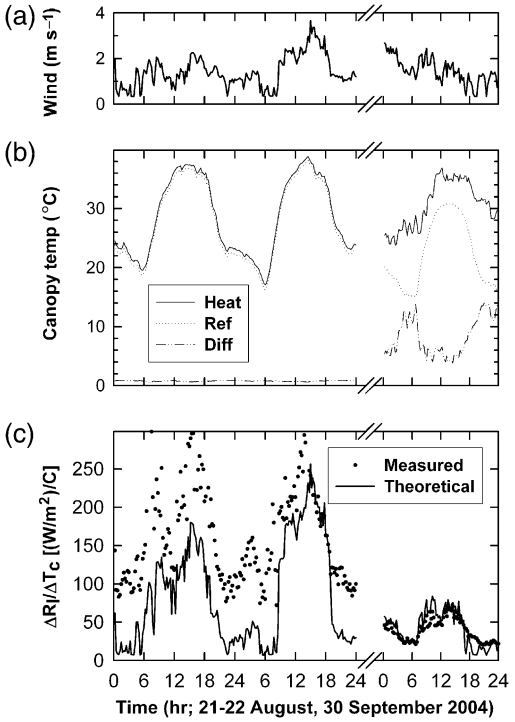

Fig. 6 (a) Fifteen-minute average wind speeds at 2 m height against time of day over 1.0 m tall Sudan grass for 21–22 August and over 0.6 m tall Sudan grass (second crop) on 30 September 2004. (b) Fifteen-minute average reference (Ref) and infrared-heated (Heat) canopy temperatures, as measured with infrared thermometers and corrected for sky and heater radiation reflected from the crop canopy. The lower curves are the temperature differences (Diff) between the heated and reference plots. The 2000 W heater was 60 cm above the top of the canopy. On 21–22 August, the heater was modulated with a PID (proportional–integrative–derivative) controller to maintain a 1.0° temperature rise of the heated plot over the reference plot, whereas on 30 September the heater was at full power all day. (c) Fifteen minute theoretical unit thermal radiation requirements ($\Delta R_l/\Delta T_c$) from Eqn (14) to change the canopy temperature of 1 m^2 of vegetation by 1 °C. For 21–22 September, the lush first-cutting crop was presumed to have canopy resistance values similar to that of an alfalfa reference crop (Walter *et al*., 2000; 30 s m^{-1} daytime and 200 s m^{-1} night-time), whereas the more sparse second-cutting crop on 30 September was assumed to have canopy resistances double those of the alfalfa reference. Also shown are the corresponding measured thermal radiation values. The measured values were determined using the PID control signal to compute electrical power consumption, which was multiplied by an efficiency factor calculated from Eqn (7) and then divided by the temperature difference between the heated and reference plots measured with the infrared thermometers.

of 1500 K, it had risen only to about 11%. Therefore, vegetation is sufficiently near black so that its reflectance ought not seriously affect the effectiveness of infrared heating.

Besides having a high reflectance for near-infrared radiation (Fig. 2), vegetation also has a high transmittance of about 50% in this portion of the spectrum (Yocum *et al.*, 1964). Therefore, any near-infrared radiation emitted by the heater would do even less than implied by Fig. 4 to warm the vegetation. However, this transmitted radiation would not be totally lost from the ecosystem because it would warm the soil, as well as the lower part of the canopy somewhat.

Performance of infrared heating system

When first deployed at a 1.5 m height above the crop canopy in a field with a set-point difference of 2 °C, the heater was on almost all the time and was unable to control the temperature of the canopy under typical daytime conditions. However, by lowering the heater to be about 60 cm above the crop (95 cm tall Sudan grass) and using a set-point difference of 1 °C, good temperature control could be achieved (Figs 5 and 6b). Sometimes the heater was fully on or fully off for several seconds, but much of the time, the heater operated within its 0–2000 W capacity, and the temperature of the heated plot deviated only a few tenths of a degree away from the set-point difference of 1 °C (Fig. 6b, retrospectively corrected for sky and heater radiation reflected from the crop canopy). The 1 °C difference could be maintained night and day, as illustrated by the left 2 days in Fig. 6b, which were more or less typical August days. For comparison, the right-hand day in Fig. 6b shows the temperature rise of the heated plot when the heater was turned full-on. The lower-right 'difference' curve shows that at night the heated plot was up to 14 °C warmer, and during the daytime, it was about 4 °C warmer. These data plus those of the heating patterns suggest that probably a height of 1.0 m could be used and still achieve controlled heating at 1 °C or alternatively, a higher set-point temperature could be used at the 60 cm height above the canopy.

Theoretical thermal radiation power requirement for raising plant canopy temperature

The energy balance of a plant canopy (neglecting photochemically fixed energy (i.e. photosynthesis and respiration)) can be written as:

$$\mathbf{R}_{sn} + \mathbf{R}_l = \mathbf{R}_c + \mathbf{G} + \mathbf{H}_c + \lambda\mathbf{ET}, \quad (8)$$

where $\mathbf{R}_{sn}$ is the net solar radiation (W m^{-2}); $\mathbf{R}_l$ is the down-coming long-wave radiation from sky + infrared heater (W m^{-2}); $\mathbf{R}_c$ is the up-going long-wave radiation from canopy (W m^{-2}); $\mathbf{G}$ is the soil heat flux (W m^{-2}); $\mathbf{H}_c$ is the sensible heat flux (W m^{-2}); $\lambda\mathbf{ET}$ is the latent heat flux from evapotranspiration (W m^{-2}), where $\mathbf{ET}$ is the evapotranspiration rate (kg m^{-2} s^{-1}); λ is the latent heat of vaporization (J kg^{-1}).

The sign convention is that the terms on the left-hand side are positive going toward the canopy surface and the terms on the right-hand side are positive going away from the surface.

The terms on the right-hand side can be expressed as:

$$\mathbf{R}_c = \varepsilon_c\sigma(T_c + 273.15)^4, \quad (9)$$

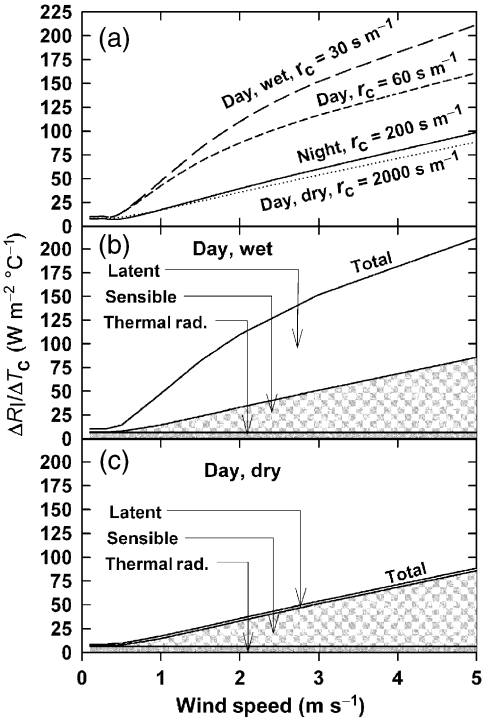

Fig. 7 (a) Theoretical unit thermal radiation power requirements ($\Delta R_l/\Delta T_c$) to change the canopy temperature per m^2 per °C of 0.5 m tall alfalfa vs. 2 m wind speed. The alfalfa crop has the same canopy resistance characteristics as the 'standardized reference evapotranspiration' equation being adopted by the American Society of Civil Engineers (Walter *et al.*, 2000). One curve is for night (solid line, zero solar radiation, unheated canopy temperature = 21 °C, air temperature = 23 °C, vapor pressure = 2.21 kPa, and canopy resistance = 200 s m^{-1}), and the other three are for daytime (solar radiation = 878 W m^{-2}, unheated canopy temperature = 35 °C, air temperature = 36 °C, vapor pressure = 1.61 kPa). For the daytime curves, canopy resistance was varied to simulate vegetation that is drought-stressed (dotted line, canopy resistance = 2000 s m^{-1}), slightly water stressed (short-dashed line, canopy resistance = 60 s m^{-1}), and amply watered (long-dashed line, canopy resistance = 30 s m^{-1}). (b) Same power requirement vs. wind speed curve (Total) as the 'Day, wet' curve in (a) but with the components due to thermal radiation and sensible and latent heat flux components shown individually. (c) Same as (b) except for the 'Day, dry' curve in (a).

which is the Stephan's Law, like Eqn (2), where ε_c is the emissivity of canopy for thermal radiation and T_c (°C) is the canopy temperature.

The sensible and latent heat fluxes can be computed using resistance equations (e.g. Rosenberg *et al*., 1983, Chapter 7).

$$\mathbf{H} = \rho c_p (T_c - T_a)/r_a, \tag{10}$$

where r_a is the aerodynamic resistance which can be calculated from wind speed, vegetation height, and air and canopy temperatures following Kimball *et al*. (1994, 1995, 1999).

$$\boldsymbol{\lambda}\mathbf{ET} = (\rho c_p/\gamma)(e_c - e_a)/(r_a + r_c), \tag{11}$$

where γ is the psychrometric constant $= (Pc_pM_a)/(\lambda M_w)$; P is the barometric pressure (kPa); M_a is the molecular weight of air (0.029 kg mol^{-1}); M_w is the molecular weight of water vapor (0.018 kg mol^{-1}); e_a is the air vapor pressure (kPa); e_c is the vapor pressure in the substomatal cavities in the leaves (kPa), which can be calculated from canopy temperature assuming saturation using Tetens' equation (e.g. Kimball, 1981; Weiss, 1977).

$$e_c = 0.61078 \exp[17.2694 T_c/(T_c + 237.30)], \tag{12}$$

where r_c is the canopy resistance to the movement of water vapor from the substomatal cavities in the leaves and from the soil through the canopy surface to the bulk air above. r_c depends on species, leaf physiology, canopy architecture, light intensity, CO_2 concentration, plant water status, and other factors. In spite of the complexity, however, engineers have had success in developing standardized reference equations for predicting the effects of weather variables on the evapotranspiration of reference grass and alfalfa canopies (Walter *et al*., 2000). For the case of a well-watered 0.5 m tall alfalfa canopy, they have adopted values of 30 and 200 s m^{-1} for day and night, respectively.

Taking derivatives with respect to T_c on both sides of Eqn (8) and using Eqns (9)–(12), and following Kimball (1981).

$$\begin{aligned} d\mathbf{R}_l = {} & 4\varepsilon_c \sigma (T_c + 273.15)^3 \, dT_c + (\rho c_p / r_a) \, dT_c \\ & + \{\rho c_p / [\gamma (r_a + r_c)]\} \\ & \times [4098.3 e_c / (T_c + 237.30)^2] \, dT_c. \end{aligned} \tag{13}$$

The derivative of **G** with respect to T_c was taken as zero. This assumption is valid because if a plot is maintained at a set temperature above a nearby control plot, then over a long time the whole soil temperature profile will adjust (e.g. Kimball & Jackson, 1979), and there will be no difference in **G** between the two plots. Of course, over short times, just after the heater is turned on, there would be an increase in **G** until the temperature profile adjusts. Similarly, the derivative of $\mathbf{R}_{sn}$ is zero because surface temperature would not directly affect short-wave solar radiation.

Rearranging Eqn (13) and changing differentials to increments,

$$\begin{aligned} \Delta\mathbf{R}_l/\Delta T_c = {} & 4\varepsilon_c \sigma (T_c + 273.15)^3 + (\rho c_p / r_a) \\ & + \{\rho c_p / [\gamma (r_a + r_c)]\} [4098.3 e_c / (T_c + 237.30)^2]. \end{aligned} \tag{14}$$

Equation (14) predicts how large an increase in downcoming infrared sky plus heater radiation power (W) will be required to produce a unit (°C) increase in canopy temperature for a unit area of land (m^2). It is the governing equation for determining the thermal radiation power needed to raise the temperature of a plot of vegetation with respect to an un-heated control plot.

The theoretical thermal radiation power requirement, $\Delta\mathbf{R}_l/\Delta T_c$, is very sensitive to wind speed as well as to canopy conductance (Fig. 7). At very low wind speed, only a few watts are needed to warm an alfalfa canopy, but at 5 m s^{-1}, more than 200 W m^{-2} C^{-1} are needed for an amply watered crop. At night, or during the day for water-stressed dry vegetation, the requirement is about half as much. The portion of $\Delta\mathbf{R}_l/\Delta T_c$ due to increased canopy thermal radiation back to the sky is relatively small (above a wind speed of about 1 m s^{-1}) and unaffected by wind speed or solar radiation (Figs 7b and c). The portion for sensible heating of the air is much larger and increases rapidly with wind speed. Likewise, the portion for latent heat increases rapidly with wind speed. Comparing Fig. 7b with 7c, the latent portion changes from day to night, as expected, using 30 and 200 s m^{-1} for r_c (Walter *et al*., 2000). During the daytime, $\Delta\mathbf{R}_l/\Delta T_c$, is quite sensitive to water stress, as indicted in Fig. 7a, comparing the curve for $r_c = 30$ with that for $r_c = 60$ s m^{-1}.

For 30 September 2004, when the heater was operated at constant full power over Sudan grass, thermal radiation efficiency as a function of wind speed was calculated from Eqn (7), multiplied by the power (2000 W), and divided by the difference in canopy temperature measured with the infrared thermometers, to determine measured values of $\Delta\mathbf{R}_l/\Delta T_c$ (Fig. 6c). Using weather data, as well as plant data in Eqn (14), theoretical values of $\Delta\mathbf{R}_l/\Delta T_c$ were also calculated. Agreement between measured and theory was excellent, both day and night. Similarly, measured and theoretical values were determined for 21–22 September 2004, when the heater was operated under PID control (Fig. 6c). The agreement was good during midday on 22 August under higher wind speeds (Fig.6a), but on 21 August and especially at night under low wind speeds the measured values tended to be about 50 W m^{-2} C^{-1} above the theoretical

curves. As a test, the 0.44 emissivity curve from Fig. 3 was used instead of Eqn (7) for radiation efficiency to calculate the measured values, but agreement between measured and theoretical in Fig. 6c was worse. Nevertheless, considering the uncertainties associated with estimating the canopy conductance of the theoretical values, with accurately measuring 1°C temperature differences between plots, and with the calculation of the radiator efficiency Eqn (7) for the measured values, the agreement is fair. Therefore, Eqn (14) ought to be adequate for estimating the thermal radiation energy requirements for heating vegetation and Eqn (7) for converting to electrical power requirements.

A procedure for first-order compensation of vapor pressure deficit effects when using infrared heaters

One identified problem for infrared heating of experimental plots is that the VPGs from inside the leaves to the air outside would not be the same as would be expected if the warming were performed by heating the air everywhere (i.e. by global warming). However, evaporation from water surfaces (whether from an open pond, films inside a leaf, or films within the soil) is a physical process which has been studied for many years, and the overall governing equations are well known. Therefore, it should be possible to compute how much water an infrared-warmed plant would lose in normal air compared with what it would have lost in air, which had been warmed at constant relative humidity, as is predicted with global warming. On an hourly or daily basis, this amount of water could be added back to plants using a drip irrigation system.

Assume that some plants are being heated by an infrared heater and canopy temperatures are known from infrared thermometer measurements, T_H for heated plants and T_R for adjacent unheated reference plants. Assume too that we have a nearby weather station from whose measurements actual air vapor pressure (e_a) and temperature (T_a) can be obtained. The problem is how to make the experiment equivalent to heating the air and maintaining constant relative humidity.

By definition:

$$RH = (e_a/e_a^*) \times 100, \quad (15)$$

where RH is the relative humidity; e_a^* is the saturation vapor pressure of the air (kPa) at air temperature (T_a).

If the air is warmed by T_H–T_A while maintaining constant relative humidity,

$$RH = (e_{aH}/e_{aH}^*) \times 100, \quad (16)$$

where e_{aH} is the vapor pressure of the heated air (kPa); e_{aH}^* is the saturation vapor pressure of the air (kPa) at an air temperature; of $T_a + (T_H–T_R)$.

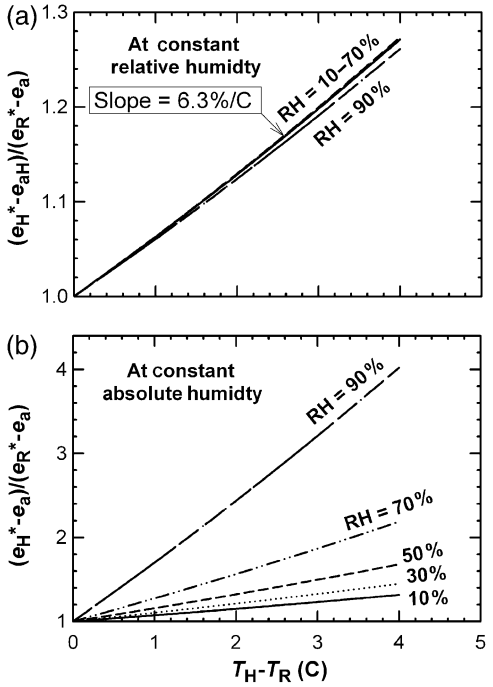

Fig. 8 Relative changes in vapor pressure gradients (and evapotranspiration rates) from infrared-heated plant canopies to the outside air vs. the temperature of the heated plots (T_H) minus that of unheated reference plots (T_R) for five values of relative humidity. These relative changes are equivalent to air heating at constant relative humidity (a) or at constant absolute humidity (b). The computations were made at a reference temperature of 30 °C, for which relative humidities of 10%, 30%, 50%, 70%, and 90% correspond to water vapor pressures of 0.42, 1.27, 2.12, 2.97, and 3.81 kPa, respectively. Note that panels (a) and (b) are not the same scale.

Combining Eqns (15) and (16),

$$e_{aH} = e_a(e_{aH}^*/e_a^*). \quad (17)$$

Thus, one can calculate the VPG from the normal reference plants to the air as:

$$VPG_R = e_R^* - e_a \quad (18)$$

and that to which the heated plants would have been exposed in air heated at constant relative humidity,

$$VPG_H = e_H^* - e_{aH}, \quad (19)$$

where e_H^* is the saturation vapor pressure inside the leaves at T_H.

For comparison purposes, the corresponding VPG for air heated at constant absolute humidity would be $e_H^* - e_a$.

In humid areas, one can assume that the reference plants are close to air temperature, but such is not generally the case and especially not in irrigated areas within an arid region. The T_R–T_a temperature difference for well-watered crops can be calculated from the

vapor pressure deficit of the air ($e^*_H - e_a$), and Idso (1982) provides empirical equations for 26 species. For the case of alfalfa, the equation is: $(T_R - T_a) = 0.51 - 1.92(e^*_a - e_a)$.

From the weather station data, a reference evapotranspiration rate, ET_o (mm h^{-1}), can be calculated, which can be multiplied by a crop coefficient, K_c, to obtain the actual evapotranspiration rate of the ambient-condition crop, ET_R (Walter *et al*., 2000; Allen *et al*., 1998). This procedure has been extensively tested and proven to be sufficiently accurate for many purposes.

Thus, to calculate the evapotranspiration rate of the heated plot if it were exposed to heated air at constant relative humidity, ET_H (mm h^{-1}), one can take:

$$ET_H = ET_R[(e^*_H - e_{aH})/(e^*_R - e_a)]. \quad (20)$$

For example, if $T_R = T_a = 30\,^\circ$C, $T_H = 32\,^\circ$C, and $e_a = 2.0$ kPa, then from Eqn (12), $e^*_R = 4.243$ kPa, and $e^*_H = 4.754$, and from Eqn (17), $e_{aH} = 2.241$ kPa. Finally, $[(e^*_H - e_{aH})/(e^*_R - e_a)] = 1.121$, or in other words, the ET rate in the heated plot would be 12% greater if instead the heating were because of a heated air treatment at constant relative humidity. For comparison, the rate of evapotranspiration while heating at constant absolute humidity would be $[(e^*_H - e_a)/(e^*_R - e_a)] = 1.228$ or 23% greater than that of the ambient reference plot.

For the case of infrared heating equivalent to air heating at constant relative humidity, the ratios of VPGs from plant to air ($(e^*_H - e_{aH})/(e^*_R - e_a)$ and thus of (ET_H/ET_R); Eqn (20)) increases at 6.3% per °C of heating over a wide range of relative humidities (Fig. 8a), and moreover, this slope is not very sensitive to absolute values of T_a or e_a (data not shown). Thus, a simple 'rule of thumb' would be to supply 6.3% more water to the heated plots per °C of warming.

In contrast, for the case of infrared heating equivalent to air heating at constant absolute humidity, the ratios of VPGs from plant to air $[(e^*_H - e_a)/(e^*_R - e_a)]$ increase rapidly with both the amount of temperature rise (T_H–T_R) and with the amount of water vapor in the air as indicated by the curves for several values of relative humidity (Fig. 8b). This is not surprising, because, for instance, if the air is very humid then ET rates will be small, and therefore when heating is carried out without humidification, the relative change in ET would be large. On the other hand, under arid conditions, ET rates are high so heating without humidification would produce a relatively smaller increase in the already large ET.

Because infrared heating of the vegetation canopy would be equivalent to air heating at constant absolute humidity, the proposed compensation procedure is to compute $ET_{Hrh} = ET_R[(e_H{}^*–e_{aH})/(e_R{}^*–e_a)]$for the constant relative humidity case, $ET_{Hah} = ET_R[(e_H{}^*–e_a)/(e_R{}^*–e_a)]$ for the constant absolute humidity case, and their difference, ET_{Hah}-ET_{Hrh} , for each period of a day (at least as short as hourly). Then these differences are summed over the number of time periods to obtain a total deficit amount of water for the day. This amount of water would be added back to the plots via a drip irrigation system early the next morning. Corrections would have to be made for any rain received and drainage below the root zone. Thereby, over seasonal time, the water status of the infrared-heated plants should approximate that of plants exposed to air heating at constant relative humidity.

Typically, for experiments for which water stress is to have no part, the reference plots are irrigated by amounts which supplement any rain in order to meet the ET requirements, and often the other plots receive the same amount of water. If elevated CO_2 is the experimental variable, such an irrigation strategy works because the elevated CO_2 plots can be expected not to have higher water requirements than the

Table 2 Estimated unit thermal radiation requirements from Eqn (14) for infrared heating of a 0.5 m tall crop of well-watered alfalfa from 1 June through 30 September 2002 at Urbana, IL, based on 10 min average weather data from the SoyFACE Project (http://www.soyface.uiuc.edu/research.htm)

Unit thermal radiation requirement (kW-h m^{-2} °C^{-1})	Unit electrical power requirement (kW-h m^{-2} °C^{-1})	Season-long thermal radiation efficiency (%)	Unit cost ($\$ m^{-2}$ °C^{-1})	Seasonal cost for 16 plots, each 16 m^2, heated by 2 °C ($)
212	1244	17.0	124	63 500

The alfalfa crop has the same canopy resistance characteristics as the 'standardized reference evapotranspiration' equation being adopted by the American Society of Civil Engineers (Walter *et al*., 2000). The unit thermal radiation requirement is the kW h of thermal radiation required per m^2 of land area and per °C rise in canopy temperature. Also shown is the estimated electrical power requirement, which was calculated from the 10 min average unit thermal radiation requirements using Eqn (7) to compute heater radiation efficiency from wind speed. The season-long thermal radiation use efficiency is the season-long thermal radiation requirement expressed as a percentage of the electrical power requirement. The unit costs ($\$ m^{-2}$ °C^{-1} at \$0.10 kW – h^{-1}) and the costs for heating 16 plots (as used for soybeans in the SoyFACE project) each 16 m^2 in area by 2 °C is also shown.

reference plots. However, if the treatment is warming by air heating at constant relative humidity, then for the above example of heating by 2 °C, to avoid water stress the plots should be irrigated so as to receive at least 12% more water (rain + irrigation) than standard. If the treatment is warming by air heated at constant absolute vapor pressure or by infrared heating, the plots should be irrigated so as to receive 23% more than standard.

Often, however, we do want water stress to be a factor in the experiments. Warming will increase ET requirements, which is an associated aspect of a warming treatment. Therefore, for this example, if infrared heating is used but we want the plants to experience water stress equivalent to air heating at constant relative humidity, the plants should be irrigated so as to receive 23%−12% = 11% more water than the reference plots.

Implementing this VPG correction procedure requires knowing the daily ET from the reference plot. As mentioned above, the ET from a standard reference crop (0.12 m grass or 0.50 m alfalfa) with an ample supply of water can be calculated from weather data using a Penman–Monteith equation following Walter *et al*. (2000) and Allen *et al*. (1998), which can then be multiplied by a crop coefficient to obtain actual ET. Utilizing soil water holding capacity data and estimated crop rooting depth, Allen *et al*. (1998) also describe how to compute the reduction in ET with developing water stress. An alternative method to estimate the effects of limited water supply which would not require soils information and which would utilize the infrared thermometer already deployed over the reference plot would be to calculate a crop water stress index from the difference between the crop canopy temperature and air temperature as a function of air vapor pressure deficit (Idso *et al*., 1981; Jackson *et al*., 1981; Idso, 1982). Besides agricultural crops with relatively uniform canopies, Allen *et al*. (1998) also present adjustments for natural plant stands using leaf area index or effective plant cover. For some experiments, however, the researcher may be able to measure actual ET rates from the reference plots using soil water balance, energy balance, Bowen ratio, eddy covariance, sap flow, weighing lysimeters, or other techniques, and of course, if the measurements can be accomplished accurately without too much disturbance of the plots, such actual measurements are to be preferred.

I have called this proposed procedure '1st order' because it will compensate for the altered VPGs from plant to air. However, the procedure will not compensate for any changes the infrared heating may have on stomatal and canopy conductances, which also modulate the ET rates. However, these conductance effects are likely to be secondary in comparison with the consequences of the plants exhausting their soil water supply earlier than would have happened with air heating with humidification.

At this time, I have no data with which to validate this procedure for water vapor gradient correction. Nevertheless, I present it in order to stimulate others who are now or are planning to conduct infrared heating experiments to test the procedure and hopefully obtain plant results more representative of those expected with global warming.

Discussion

Infrared heater efficiency

The manufacturer targets indoor applications for their sales, which is appropriate. However, for the outdoor T-FACE case, there is a major conflict between decreasing heater efficiency (Fig. 3) and increasing vegetation power requirement (Fig. 7) as wind speed increases. Previous authors have not presented thermal radiation efficiency data for their infrared heaters, but for three of the projects, I was able to deduce their efficiencies from information in their papers (Table 1). The efficiencies ranged from 11% to 27%, which is reasonably consistent with what one would expect from Fig. 3 for typical outdoor wind speeds. As will be presented in a later section, using Eqn (7) with weather data for June–September 2002 from Urbana, IL, produced a season-long estimate of 17.0% efficiency for that site (Table 2).

Of course, the heater performance data presented herein only directly applies to the incoloy-sheathed, open-air, rod-type heater used in this study, which was selected because it is the type used in most prior experiments (all except Nijs *et al*. (1996) and Shaw *et al*. (2002) in Table 1). Other heater designs would have different performance, which invites speculation about what would be an ideal design for this open-field, free-air ecosystem heating application. Some possible improvements include the following:

1. Make the heating element more black. From Fig. 3, it appears that efficiency would double if the heating element surface emissivity were increased from 0.44 to 1.00.
2. Put a window cover across the opening on the underside of the cover to minimize convective loses because of the wind. This could result in a huge increase in efficiency (Fig. 3). This window would need to be transparent to long-wave radiation (> 850 nm), yet be able to tolerate the high temperatures of the heater.
3. Reduce the size of the housing and reflector to a minimum to reduce solar radiation shading effects.

4. Operate at hotter temperatures so as to have a more powerful heater for the same physical size, which could then be deployed higher above the canopy and warm a larger area. However, hotter temperatures would likely lead to more emissions in far-red portion of the spectrum, which are absolutely undesirable because they would be phytochromatically active, and also more in the near-infrared, which would be less effective for heating vegetation because vegetation has greater reflectance for near-infrared (Figs 2 and 4). Nijs *et al*. (1996) had a more powerful heater (Table 1), for which they installed additional filters to remove energy at wavelengths less than 800 nm. However, their Schott RG 850 filter also cuts out wavelengths longer than 2700 nm (http://www.besoptics.com/html/body_schott_rg850_filter_glass.html), which would eliminate some desired thermal radiation (Fig. 2), and therefore would reduce efficiency. On the other hand, such a filter would have shielded the heater element from the wind (see #2 above), so it is possible that they achieved a high efficiency in spite of removing some of the emitted energy with the filters. Even though their heater might have been efficient, nevertheless it appears quite bulky in the photograph in their paper, and they avoided severe solar radiation shading problems only because they worked with a tiny plot (0.2 m^2) at a relatively high latitude (47°N) site.

Thermal radiation power requirement for warming plant canopies and heater system performance

Except for Nijs *et al*. (1996), all the other experimenters listed in Table 1 have not used active PID or other control of the output of the their infrared heaters. Therefore, for these uncontrolled heaters, the output decreased with increasing wind speed (Fig. 3) just as the power requirement for warming the vegetation increased (Fig. 7). As a consequence, the vegetation in their experiments must have experienced a much more drastic treatment under calm conditions at night and almost none at all during turbulent daytime conditions, similar to the 30 September data in Fig. 6b. In fact, Wan *et al*. (2002) show a dramatic decrease in their mostly mid-canopy heated-minus-control air temperature differences with increasing wind speed. They also reported that their average increase in daily maximum canopy air temperature because of infrared heating was only 0.1 °C, whereas the increase in daily minimum temperatures was 2.3 °C. Thus, except for Nijs *et al*. (1996), these previous studies have had treatments that were primarily just night-time heating. To some extent this can be justified because night-time minimum temperatures are predicted to warm more than daytime maximums in the future (IPCC, 2001). Nevertheless, the warming treatment imposed by uncontrolled infrared heaters does not appear to be able to warm vegetation very much like that expected in the future.

Similar to Nijs *et al*. (1996) and in contrast to the other studies, the heater control system described herein was able to provide a precisely controlled increase in temperature of the heated plot above that of the reference plot almost all the time (21–22 August data in Fig. 6b). Indeed, a next logical test of our system would be to raise the heater (and thereby heat a larger area) until the performance falls below some criteria such as the 15 min average temperature differences should be within 0.1 °C of the set-point difference 90% of the time.

One consistent effect of infrared heating in the prior experiments has been an increase in soil temperatures (Table 1). Such increases in soil temperature would affect the rates of most soil processes, so besides the vegetation temperatures, it is very important that the soil temperatures in global warming experiments also be representative of the likely future conditions. For the case of a complete canopy cover, the largest fluxes of energy are exchanged in the canopy above the soil surface. Therefore, if experimenters force the vegetation temperatures to be correct, the soil temperatures will follow and also be correct (assuming that VPGs and water use are accounted as discussed in the previous section). For the case of bare soil and snow surfaces, if the canopy resistance (r_c, Eqn (11)) is reinterpreted as a surface resistance with appropriate formulas for evaluation, Eqn (14) still ought to be applicable for estimating the unit thermal radiation requirement to raise the soil or snow temperatures. However, for the case of sparse canopies with incomplete canopy cover, the theory would be difficult to apply because of the difficulty in measuring the proper representative canopy temperatures.

A sample use of Eqn (14) to predict operating costs for infrared heating of subplots within the main plots of the SoyFACE Project

As already discussed, Eqn (14) can be used to predict the thermal radiation power required to warm plant canopies from weather data and plant characteristics, and it gave fair agreement with measured values (Fig. 6c). For some canopies, such as the sparse and inhomogeneous montane vegetation studied by Harte *et al*. (1995) in uneven topography, it is difficult to estimate plant height and canopy resistance and to accurately calculate aerodynamic resistance from wind speed. Nevertheless, for many ecosystems, especially

agricultural crops, Eqn (14) should be sufficiently accurate to design infrared heating experiments.

For example, the SoyFACE project at Urbana, IL, has sixteen 18 m-diameter circular plots of soybeans in which there are four replicates each of ambient, elevated CO_2, elevated O_3, and elevated $CO_2 + O_3$ treatments. Equation (14) was used to estimate the cost for infrared heating subplots within the main circular plots, assuming the soybeans would not be water-stressed and would have evapotranspiration similar to that of a reference alfalfa crop (Walter *et al*., 2000) all season long. Weather data observed at 10 min intervals from 1 June through 30 September 2002 were downloaded from the SoyFACE web site (http://www.soyface.uiuc.edu/research.htm), and the unit thermal radiation requirement was calculated from Eqn (14) for each 10 min period, amounting to 212 kW-h m^{-2} $°C^{-1}$ for the 4-month growing season (Table 2). Next the electrical power requirement was calculated for each 10 min period using an efficiency factor based on wind speed from Eqn (7), which amounted to 1244 kW-h m^{-2} $°C^{-1}$. Thus, the theoretical overall seasonal average thermal radiation efficiency for the heater under Urbana, IL, conditions would be about 17.0%. Assuming electrical power costs \$0.1 $kW-h^{-1}$, the seasonal unit operating cost would be \$124 m^{-2} $°C^{-1}$. Assuming further that the desired temperature rise of the heated plots is 2 °C and that the subplots would be squares 4 m on a side (16 m^2), the seasonal power cost for infrared heating of the 16 plots would be about \$63,500 (Table 2).

Conclusions

1. The infrared heating system with PID controller and infrared thermometers was able to maintain a constant set-point temperature difference between heated and reference plots very well, provided the heater was not too high above the vegetation.
2. The thermal radiation efficiency of the heater was about 20% in free-air and decreased with increasing wind speed.
3. However, the decrease in efficiency with wind speed could be adequately estimated by Eqn (7).
4. Equation (14) was able to predict the unit thermal radiation-heating requirement of vegetation fairly well from weather data and plant characteristics, although measured values were higher than theoretical when operated at a PID-controlled 1°C temperature rise under low wind speeds especially at night.
5. A first-order correction to the VPG problem should be possible by (a) calculating how much water an infrared-warmed plant would lose in normal air compared with what it would have lost in air which had been warmed at constant relative humidity, as is predicted with global warming and then (b) irrigating with this amount of water.

Acknowledgements

The skilled technical assistance of Mathew Conley in assembling the heater system, deploying it in the field, and obtaining the data is gratefully acknowledged. I am also grateful to Kevin Martin and Dean Pettit for their help with the power connections and measurements. My colleagues, Glenn Fitzgerald and Paul Pinter, obtained the spectral irradiance data and provided helpful comments. Andrew French similarly provided helpful comments and an empirical equation for estimating 6.5 to 14 μm sky radiation. Tom Clarke assisted with the micrometeorological measurements and infrared thermometer calibrations. I appreciate the advice of John Harte and the hospitality of the Rocky Mountain Biological Laboratory, Gothic, CO, at the outset of this study. The furnishing of the PID controller code gratis by Campbell Scientific, Logan, UT, and other measurement advice is also greatly appreciated. Bruce MacDoughall, Kalglo Electronics, provided helpful information about their heater. This paper was significantly improved by the comments of three anonymous reviewers.

References

Allen RG, Pereira LS, Raes D *et al*. (1998) *Crop Evapotranspiration: Guidelines for Computing Crop Water Requirements, FAO Irrigation and Drainage Paper 56*. Food and Agriculture Organization of the United Nations, Rome, Italy (Also http://www.fao.org/docrep/X0490E/x0490e00.htm).

Bridgham SD, Pastor J, Updegraff K *et al*. (1999) Ecosystem control over temperatures and energy flux in northern peatlands. *Ecological Applications*, **9**, 1345–1358.

Campbell GS (1977) *An Introduction to Environmental Biosphysics*. Springer-Verlag, New York, NY.

Drake BG, Rogers HH, Allen Jr LH (1985) Methods of exposing plants to elevated carbon dioxide. In: *Direct Effects of Increasing Carbon Dioxide on Vegetation, DOE/ER-0238* (eds Strain BR, Cure JD), pp. 11–31. United States Department of Energy, Washington DC, USA.

Harte J, Shaw R (1995) Shifting dominance within a Montane vegetation community: results of a climate-warming experiment. *Science*, **267**, 876–880.

Harte J, Torn MS, Chang F-R *et al*. (1995) Global warming and soil microclimate results from a meadow-warming experiment. *Ecological Applications*, **5**, 132–150.

Hendrey GR (1993) *Free-air Carbon Dioxide Enrichment for Plant Research in the Field*. C.K. Smoley, Boca Raton, FL.

Hillier SH, Sutton F, Grime JP (1994) A new technique for the experimental manipulation of temperature in plant communities. *Functional Ecology*, **8**, 755–762.

Idso SB (1982) Non-water-stressed baselines: a key to measuring and interpreting land water stress. *Agricultural Meteorology*, **27**, 59–70.

Idso SB, Jackson RD, Pinter PJ Jr *et al*. (1981) Normalizing the stress-degree-day parameter for environmental variability. *Agricultural Meteorology*, **24**, 45–55.

Ineson P, Benham DG, Poskitt J *et al*. (1998) Effects of climate change on nitrogen dynamics in upland soils. 2. A warming study. *Global Change Biology*, **4**, 153–161.

IPCC (2001) *Climate Change 2001: The Scientific Basis, Contribution from Working Group I to the Third Assessment Report, Inter-governmental Panel for Climate Change* (eds Houghton JT, Ding Y, Griggs DJ, Noguer M, Van der Linden PJ, Dai X, Maskell K, Johnson CA), Cambridge University Press, Cambridge, UK.

Jackson RD, Idso SB, Reginato RJ *et al*. (1981) Canopy temperature as a crop water stress indicator. *Water Resources Research*, **17**, 1133–1138.

Kimball BA (1981) Rapidly convergent algorithm for non-linear humidity and thermal radiation terms. *Transactions of the ASAE*, **24**, 1476–1477, 1481.

Kimball BA, Jackson RD (1979) Soil heat flux. In: *Modification of the Aerial Environment of Plants. Monograph No. 2* (eds Barfield BJ, Gerber JF), pp. 211–219. American Society of Agricultural Engineers, St. Joseph, MI.

Kimball BA, Kobayashi K, Bindi M (2002) Responses of agricultural crops to free-air CO2 enrichment. *Advances in Agronomy*, **77**, 293–368.

Kimball BA, LaMorte RL, Pinter PJ Jr *et al*. (1999) Free-air CO_2 enrichment (FACE) and soil nitrogen effects on energy balance and evapotranspiration of wheat. *Water Resources Research*, **35**, 1179–1190.

Kimball BA, LaMorte RL, Seay RS *et al*. (1994) Effects of free-air CO_2 enrichment on energy balance and evapotranspiration of cotton. *Agricultural and Forest Meteorology*, **70**, 259–278.

Kimball BA, Pinter PJ Jr, Garcia RL *et al*. (1995) Productivity and water use of wheat under free-air CO_2 enrichment. *Global Change Biology*, **1**, 429–442.

Kimball BA, Pinter PJ Jr, Wall GW *et al*. (1997) Comparisons of responses of vegetation to elevated carbon dioxide in free-air and open-top chamber facilities. In: *Advances in Carbon Dioxide Research* (eds Allen LH Jr, Kirkham MB, Olszyk DM, Whitman CE), pp. 113–130. American Society of Agronomy, Crop Science Society of America, and Soil Science Society of America, Madison, WI.

Luo Y, Wan S, Hui D *et al*. (2001) Acclimatization of soil respiration to warming in tallgrass prairie. *Nature*, **413**, 622–625.

McLeod AR, Long SP (1999) Free-air carbon dioxide enrichment (FACE) in global change research: a review. *Advances in Ecological Research*, **28**, 1–56.

Noormets A, Chen J, Bridgham SD *et al*. (2004) The effects of infrared loading and water table on soil energy fluxes in northern peatlands. *Ecosystems*, **7**, 573–582.

Nijs I, Kockelbergh F, Teughels H *et al*. (1996) Free air temperature increase (FATI): a new tool to study global warming effects on plants in the field. *Plant, Cell and Environment*, **19**, 495–502.

Pinter PJ, Kimball BA, Wall GW *et al*. (2000) Free-air CO_2 enrichment (FACE): blower effects on wheat canopy microclimate and plant development. *Agricultural and Forest Meteorology*, **103**, 319–333.

Peresta GJ, Kimball BA, Johnson SM (1991) *Procedures for CO_2-Enrichment chamber construction and data acquisition and analysis, WCL Report 18*. U.S. Water Conservation Laboratory, USDA-ARS, Phoenix, AZ.

Rosenberg NJ, Blad BL, Verma SB (1983) *Microclimate: the biological environment*. Wiley-Interscience, New York.

Salisbury FB, Ross CW (1992) Chapter 20, Photomorphogenesis. In: *Plant Physiology* (eds Salisbury FB, Ross CW), 4th edn. pp. 438–443. Wadsworth Publishing, Co., Belmont, CA.

Shaver GR, Canadell J, Chapin FS III *et al*. (2000) Global warming and terrestrial ecosystems: a conceptual framework for analysis. *Bioscience*, **50**, 871–882.

Shaw MR, Zavaleta ES, Chiariello NR *et al*. (2002) Grassland responses to global environmental changes. *Science*, **298**, 1987–1990.

Shen KP, Harte J (2000) Ecosystem climate manipulations. In: *Methods in Ecosystem Science* (eds Sala OE, Jackson RB, Mooney HA, Howarth RW), pp. 353–369. Springer, New York, NY.

Walter IA, Allen RG, Elliott R *et al*. (2000) ASCE's standardized reference evapotranspiration equation. In: *National Irrigaton Symposium, Proceedings of the 4th Decennial Symposium* (eds Evans RG, Benham BL, Trooien TP), pp. 209–214. American Society of Agricultural Engineers, St. Joseph, MI.

Wan S, Luo Y, Wallace LL (2002) Changes in microclimate induced by experimental warming and clipping in tallgrass prairie. *Global Change Biology*, **8**, 754–768.

Weiss A (1977) Algorithms for the calculation of moist air properties on a hand calculator. *Transactions of the ASAE*, **20**, 1133–1136.

Williams CDH (2003) *Feedback and Temperature Control*. School of Physics, University of Exeter, http://Newton.ex.ac.uk/teaching/CDHW/Feedback/

Yocum CS, Allen LH, Lemon ER (1964) Photosynthesis under field conditions. VI. Solar radiation balance and photosynthetic efficiency. *Agronomy Journal*, **56**, 249–253.